CFD Simulation using FLUENT and RANS3D – A validation exercise

1. Introduction

In the recent past Computational Fluid Dynamics (CFD) is being extensively used both in the design phase to select the configuration and in the production phase to analyze its performance. Several commercial CFD packages are available for analysing of internal and external flows to cater the need of aerospace, automobile and process industries. These packages are usually integrated systems which include a mesh generator, a flow solver, and a visualization tool. The numerical techniques adopted in these CFD codes are well accepted algorithms published in the open literature which are robust, reliable and validated for different class of problems. In the recent past, there have been few attempts in the literature to access the relative performance of these codes (Gianluca Iaccarino 2000).

The present study aims at two-dimensional numerical simulation of some benchmark problems using the in-house flow solution code RANS3D and the commercially available FLUENT code and the results obtained using these codes are compared with available measurement and/or other computations. Two-dimensional computations have been carried out for (i) laminar flow in a lid-driven square cavity (ii) turbulent flow past a backward facing step and (iii) turbulent flow past an aerofoil by solving incompressible Navier Stokes equations. The turbulent flow simulations have been carried out by solving the Reynolds Averaged Navier Stokes (RANS) equations coupled to eddy-viscosity based Shear Stress Transport (SST) model (Menter 1994) and one-equation Spalart & Allmaras (SA) model (Spalart & Allmaras 1992).

1.1 Documentation outline

The present document consists of five different sections starting with this introduction as the first one. Section 2 describes in brief the in-house grid generation procedure and GAMBIT the pre-processor of FLUENT used to generate the body-fitted grids for the present simulation. The brief description of the flow solver RANS3D and FLUENT used for the present simulation are described in Section 3. The results and discussions are presented in section 4 and section 5 provides the concluding remarks, followed by the references.

2. Numerical Grid Generation Procedure

2.1 Mesh generation for in-house flow-solver

The in-house structured grid generation algorithm (Fathima *et al* 1994) developed at the CTFD Division, NAL involves the solution of the elliptic type differential equations at a coarser level, followed by simple algebraic interpolation from a coarser level to a finer level.

2.2 Mesh generation for FLUENT solver

GAMBIT (Ansys Inc 2009) is a software package designed to generate structured as well as unstructured mesh required for CFD analysis. GAMBIT software has been used to generate the structured grid for FLUENT simulations for all the three-benchmark problems.

3. Mathematical Modeling

3.1 Numerical solution for finite volume equations used in RANS3D solver

The RANS3D code developed at CTFD division NAL (Majumdar *et al* 2010), Bangalore is based on an implicit finite volume algorithm to solve the time-averaged Navier-Stokes equations for unsteady incompressible turbulent flow with moving boundaries in an inertial frame of reference. This general purpose time–accurate flow solver uses multiblock structured non-orthogonal boundary-fitted curvilinear grids for collocated variable arrangement with cartesian velocity components as dependent variables. The solver employs an iterative decoupled pressure-velocity solution approach similar to the SIMPLE algorithm (Patankar 1971) but modified for collocated variable arrangement using the momentum interpolation strategy (Majumdar 1988) in order to avoid the checkerboard oscillations of the flow variables. The system of linear equations derived from the finite volume procedure is solved sequentially for the velocity components, pressure correction and turbulent scalars using the strongly implicit procedure (Stone 1968). The code is coupled a wide spectrum of state-of-the-art eddy viscosity based turbulence models. The code is extensively validated for wide variety of problems related to naval hydrodynamics and low speed aerodynamics.

3.2 Brief description about FLUENT software

FLUENT (Ansys Inc 2009) is a commercial CFD software package. It is a fluid flow solver which can analyse the different flow regimes (subsonic to supersonic). The flow solver can handle structured, unstructured and hybrid meshes (combination of structured and unstructured grids). FLUENT solves the incompressible (subsonic) flows using the pressure based approach and compressible flows (high speed flows) using the density based approach. The present incompressible flow analysis is carried out using the pressure based method which follows the SIMPLE algorithm (Patankar 1971).

4. Results and Discussions

4.1 Laminar flow in a lid driven square cavity

4.1.1 Motivation

Development of laminar flow in a lid-driven square cavity is a work-horse problem often used for validation of a CFD code/algorithm. Here the flow is confined from all four sides and is an example of a recirculating flow induced by the moving the top lid (wall) with the other three walls at rest. Although the geometrical and physical boundary conditions are simple and unambiguous, the physics of such strongly recirculating flow however is quite complex. The present laminar flow computations carried out using RANS3D and FLUENT have been compared with the available computational data (Ghia et *al* 1982).

4.1.2 Computational details

A simple cartesian grid has been used to discretize the unit length two-dimensional square cavity. The laminar computation has been carried out for a flow Reynolds number of 100 based on the cavity length (L) and lid velocity (U_{lid}). The grid and boundary condition used for both FLUENT and RANS3D simulations are shown in Fig.4.1. The computational flow domain is covered by 101 × 101 grid nodes. Both the computations use the third order accurate QUICK scheme for the convective flux discretisation with the convergence criteria of 10^{-4}.

4.1.3 Velocity distribution and flow pattern

Fig. 4.2 compares the velocity profiles obtained from the present RANS3D and FLUENT computations with the computational data of Ghia and Ghia, 1982. The transverse distribution of non-dimensionalised longitudinal velocity (u/U_{lid}) at x/L=0.5 and the longitudinal distribution of transverse velocity (v/U_{lid}) at y/L=0.5 obtained using both the commercial and the in-house solvers shows an excellent agreement against the available computational data. The streamlines patterns obtained by the RANS3D and FLUENT (Fig 4.3) are observed to be realistic and identical.

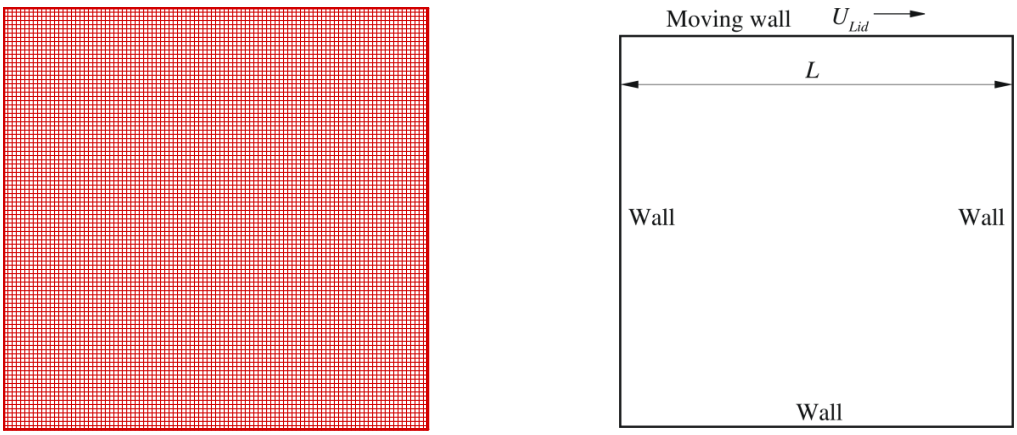

(a) Computational grid : 101x101 (b) Boundary conditions

Figure 4.1: Grid and boundary condition for lid driven square cavity

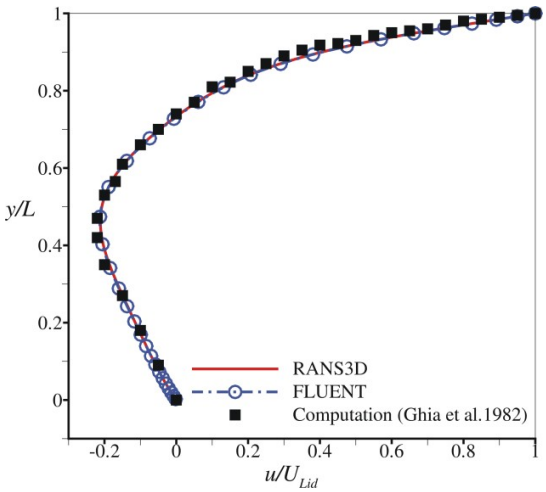

(a) Transverse distribution of longitudinal velocity at x/L=0.5

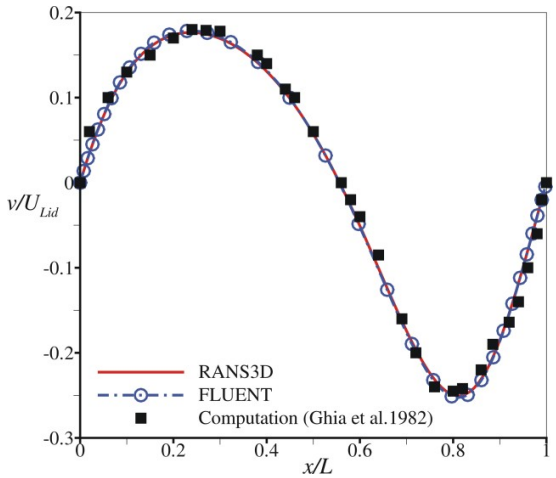

(b) Longitudinal distribution of transverse velocity at y/L=0.5

Figure 4.2: Computed velocity profiles obtained using RANS3D and FLUENT for laminar flow in a lid driven square cavity (Re =100)

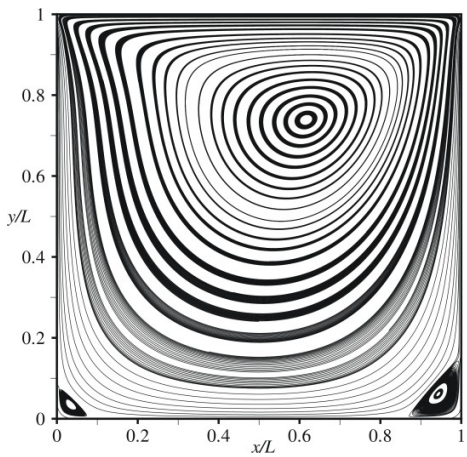

(a) Streamlines obtained using RANS3D

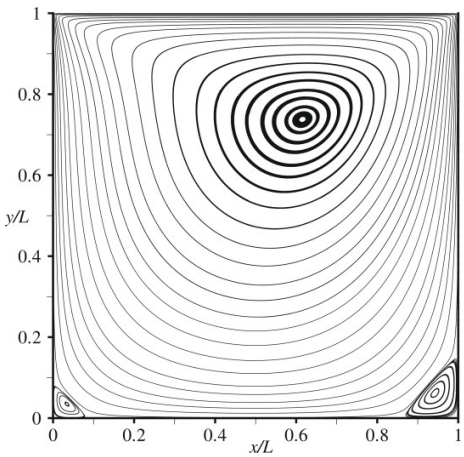

(b) Streamlines obtained using FLUENT

Figure 4.3: Computed streamlines obtained using RANS3D and FLUENT for laminar flow in a lid driven square cavity (Re =100)

4.2 Turbulent flow past a backward facing step

4.2.1 Motivation

Separation and reattachment of turbulent flows occur in many practical engineering applications, both in internal flow systems such as diffusers, combustors and channels with sudden expansions, and in external flows like those around airfoils and buildings. In these situations, the flow experiences an adverse pressure gradient, *i.e.* the pressure increases in the direction of the

flow, which causes the boundary layer to separate from the solid surface. The flow subsequently reattaches downstream forming a recirculation bubble. In the present work, flow past a backward facing step has been carried out for a Reynolds number of 5000 based on the step height (*h*). The results obtained from both RANS3D and FLUENT simulations are compared with the measurement data (Jovic *et al* 1994) for reattachment length and the skin friction distribution.

4.2.2 Computational details

The two-dimensional computational grid and boundary conditions along with the details of the computation domain used for the backward facing step are shown in Fig. 4.4 and Fig 4.5 respectively. The boundary condition used for the present FLUENT simulation is similar to that used for RANS3D simulation except at the exit boundary. At the exit boundary, for RANS3D computation the streamwise gradients are made zero ($d\varphi/dx=0$) whereas for FLUENT the pressure-outlet condition (uses the given static pressure at the outlet plane) has been used. The cartesian grid (Fig. 4.4 (a) and 4.4(b)) generated for the present simulation consists of 201x201 grid nodes with the grids stretched towards both the horizontal and the vertical walls of the step in order to resolve the sharp gradients (near wall $y^+<1$, where $y^+$is the non-dimensional wall distance $= yu_\tau/\nu$). Both the simulations have been carried out using third order accurate QUICK scheme for the convective flux discretisation and the effect of turbulence has been modeled using two turbulence models *viz.*, SA and SST. Uniform inlet profile of the mean velocity has been prescribed at a longitudinal station 10h upstream of the vertical wall of the step and the turbulence energy at the inlet plane is assumed to be 10^{-4} times the mean kinetic energy. The eddy viscosity is assumed to be 10 times the laminar viscosity of the fluid.

(a) Full view of the grid (201x201)

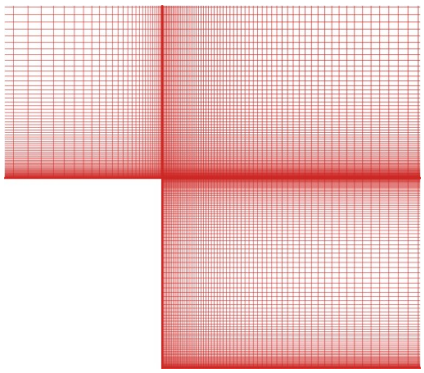

(b) Zoomed view of the grid near the step

Figure 4.4: Numerical grid for the flow past a backward facing step

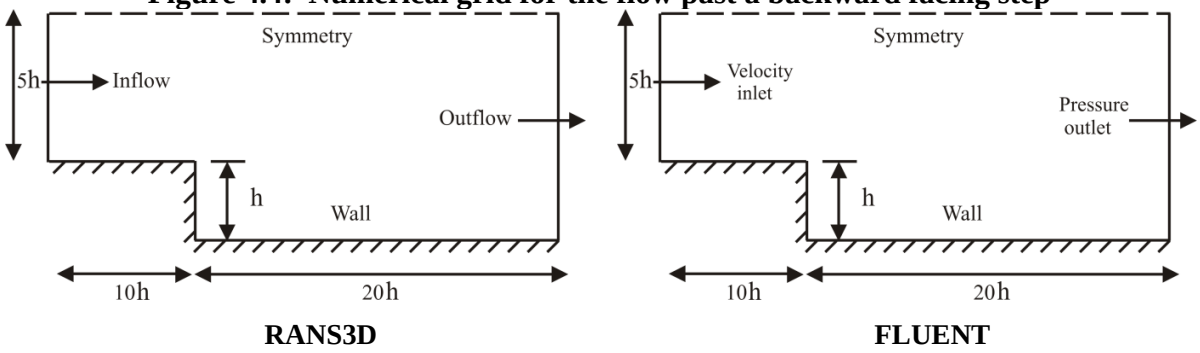

Figure 4.5: Boundary conditions for the flow past a backward facing step

4.2.3 Skin friction coefficient and flow pattern

The distribution of the skin-friction coefficient ($C_f = \tau_\omega / 0.5\rho U_\infty^2$) along the bottom wall of the step obtained by both the simulations using the SA and SST turbulence models are shown in Fig 4.6. The double change of sign in the skin friction distribution clearly indicates the presence of a large recirculation bubble preceded by another very small bubble near the step corner. The SA model in both the solvers overpredicts the C_f value before reattachment and closely follows the measurement results in the post reattachment region. On the other hand, the RANS3D prediction using SST turbulence model is observed to have closer agreement with the measurement data especially for the peak C_f whereas the SST of FLUENT overpredict the C_f. The particle trace clearly indicating the separated and reattachment region for the computed flow field using different turbulence models are shown in Fig 4.7 and Fig 4.8. The reattachment length for different turbulence models for both the solvers has been compared with the measurement data as shown in Table 4.1, clearly shows that the predictions of SA model of RANS3D and SST model of FLUENT are closer to the measurement data as compared to other two computational results.

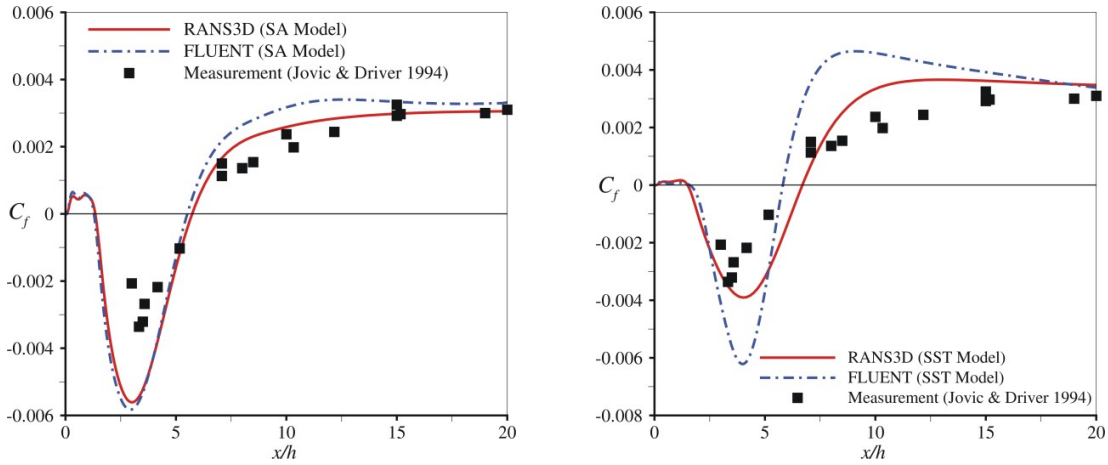

(a) SA Model (b) SST Model

Figure: 4.6: Variation of skin-friction coefficient along the bottom-wall for backward facing step using different turbulence models (Re=5000)

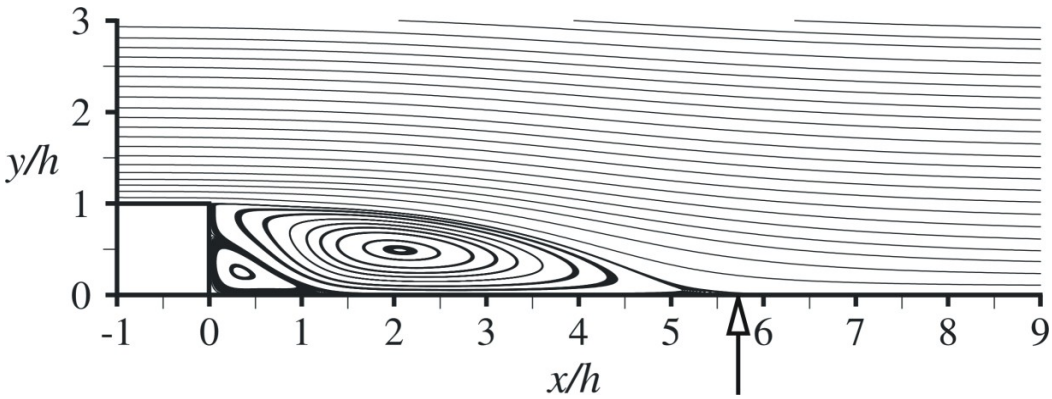

(a) RANS3D

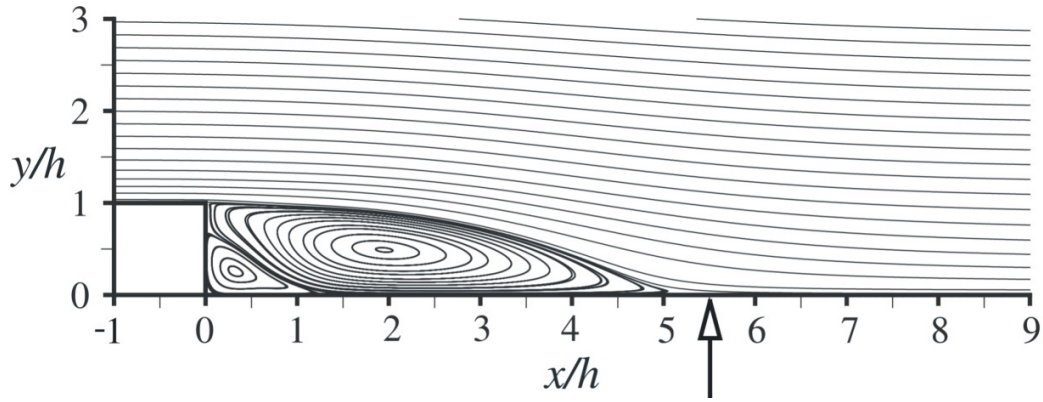

(b) FLUENT

Figure 4.7: Computed streamlines for backward facing step using SA model (Re=5000)

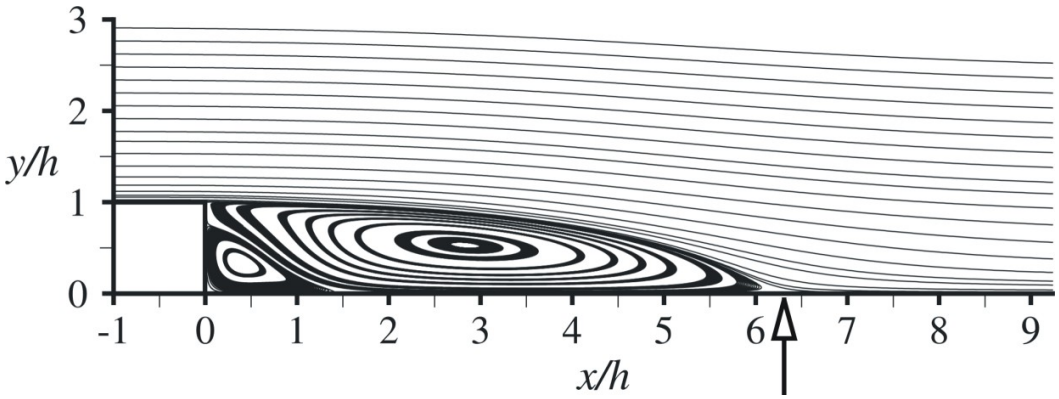

(a) RANS3D

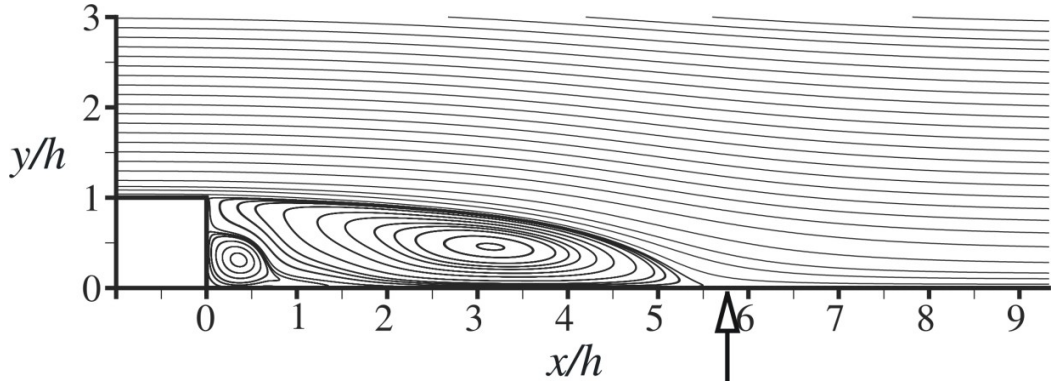

(b) FLUENT

Figure: 4.8: Computed streamlines for backward facing step using SST model (Re=5000)

	SA Model	SST Model
RANS3D	5.7364	6.3
FLUENT	5.5146	5.8
Measurement (Jovic & Driver, 1994)	6±0.15	

Table 4.1: Comparison of reattachment length for backward facing step obtained from present computation using for two different turbulence models (Re=5000)

4.3 Turbulent flow past NACA0012 aerofoil

4.3.1 Computational details

Two block C-grid (Fig. 4.9) consisting of 526 × 100 control volumes (CV) has been employed for RANS3D simulations. A single block C-grid (Fig. 4.10) having the same number of CV's for the FLUENT simulations. In both the cases the far field is placed at a radius of 15*C*, where *C* is the chord length of the aerofoil. In order to resolve the sharp flow gradients, the grid lines are stretched towards the aerofoil boundary so that the y^+ is maintained to be less than 1 in both the cases. The third order accurate QUICK scheme for convective flux discretisation coupled to SA and SST turbulence models have been used for the present computations. The typical boundary conditions used for the present RANS3D simulation are shown in Figure 4.11. The farfield is treated either as an inflow where the flow is prescribed or as an outflow boundary condition depending on the sign of the convective flux on the relevant face. At the aerofoil wall, the velocity components are set to zero, the convective and diffusive fluxes across the boundary are delinked and the wall shear effect is simulated through appropriate source terms in the momentum equations. At the block (cut) boundary, one overlapping control volume is provided on the either side of the block interface boundary for appropriate transfer of the solution from the neighbouring block. The boundary conditions used in the FLUENT analysis for single-block grid (Fig. 4.12) are as follows: (i) on the outer curved and the horizontal surfaces of the domain the velocity Inlet condition was specified, (ii) on the outer vertical surfaces of the domain pressure outlet boundary condition was specified with the outlet pressure being atmospheric pressure and (iii) on the airfoil surface a no-slip condition was specified . The results obtained are compared for mean aerodynamic coefficients and mean surface pressure distributions with available measurement data (Charles 1981).

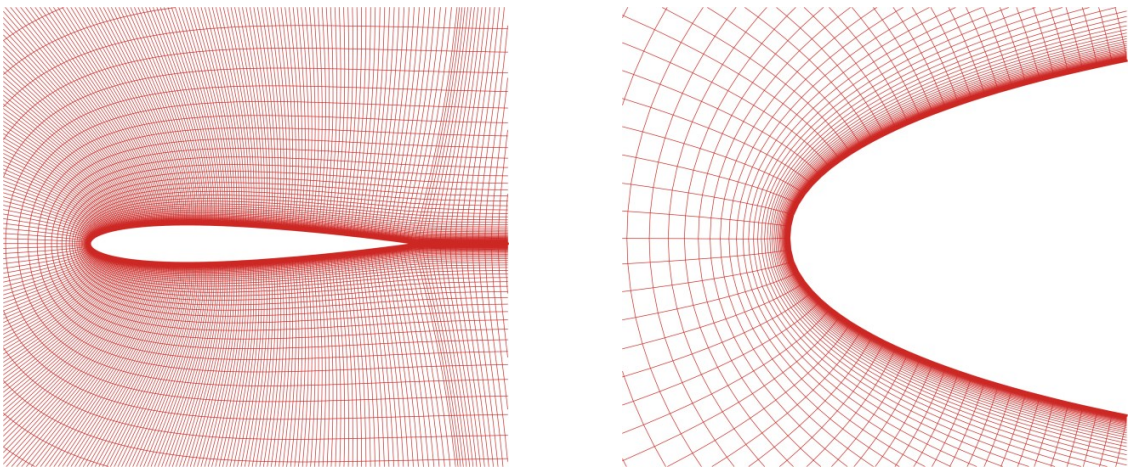

(a) Grid near the Airfoil (b) Zoomed view near the Leading edge

Figure 4.9: Numerical Grid around NACA0012 airfoil (527 x101) for RANS3D computation

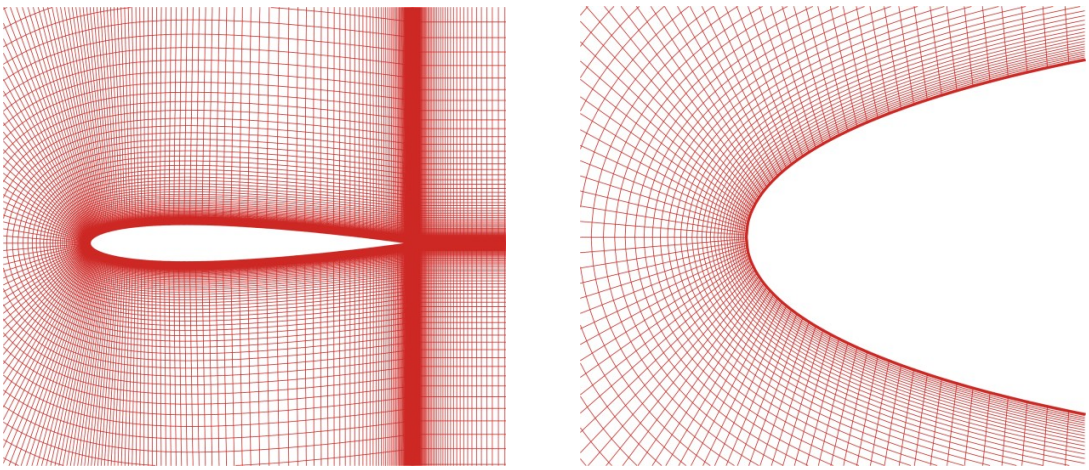

(a) Grid near the Airfoil (b) Zoomed view near the Leading edge

Figure 4.10: Numerical Grid around NACA0012 airfoil (527 x101) for FLUENT computation

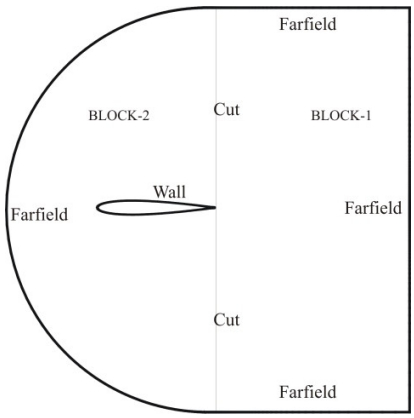

Figure 4.11:Boundary conditions for flow past NACA0012 airfoil used for RANS3D computations

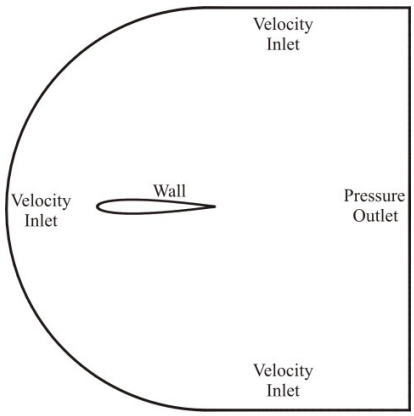

Figure 4.12:Boundary conditions for flow past NACA0012 airfoil used for FLUENT computations

4.3.2 Surface pressure distribution and flow pattern

Fig. 4.13 and Fig 4.14 (shows the computed) compares the computed surface pressure distribution ($C_p = (p - p_\infty)/0.5\rho U_\infty^2$) over the aerofoil at four different angles of attack (α) using RANS3D and FLUENT with the available measurement data. Both the solvers using two turbulence models (SA and SST) show a reasonably good agreement with the measurement data at different angles of attack. However the suction peak is slightly overpredicted by the present simulations. The streamlines computed from time integration of the velocity field at four different angles of attack for SA and SST models are shown in Fig.4.15 and Fig.4.16. The streamlines patterns obtained by both solvers for two different turbulence models are almost identically at all the angles of attack. These plots clearly show the gradual bending of the streamlines near the aerofoil surface as the angle of attack increases. A small separation bubble is observed on the upper surface near the trailing edge at $\alpha = 16^o$ in both turbulence models for both the codes. Beyond this the separation bubble gradually grows in size and spreads over the upper surface as shown in the figure for $\alpha = 20^o$.

4.3.3 Aerodynamic coefficients

The aerodynamic coefficients like the lift (C_l) and drag (C_d) coefficients can easily be computed from the numerical integration of the surface forces *viz.*, the pressure acting normal to the surface and the shear stress acting along the surface. The drag and the lift coefficients represent the resultant forces on the aerofoil along the flow and normal to the flow direction respectively, non-dimensionalised by the product of the dynamic head and the aerofoil chord length which is the projected area of the curved aerofoil on which the surface forces act. The variation of aerodynamic coefficients with angle of attack obtained by the two solvers using SA and SST turbulence models are shown in Fig. 4.17 and Fig 4.18 respectively. The variation of the aerodynamic coefficients with α for both the turbulence models are observed to follow the expected trend and matches well with measurement data especially at lower angle of attacks ($\alpha \leq 10^o$). The maximum lift for the two turbulence model is observed at 16^0 for both the RANS3D and FLUENT solvers as compared to measurement data of 15^0 with the value of maximum lift for RANS3D being closer to the measurement data. The variation of drag coefficient is shown in fig 4.17(b) and

4.18(b). The plot clearly shows that the C_d obtained by the FLUENT simulation for SA turbulence model having a better agreement with the measurement. From Fig 4.17(c) and Fig 4.18(c) it is clear that C_m obtained using RANS3D having a closer agreement with the measurement. Even though both RANS3D and FLUENT predict the stall angle later by 1^0 as compared to measurement data the overall prediction of RANS3D has better agreement with the measurement data.

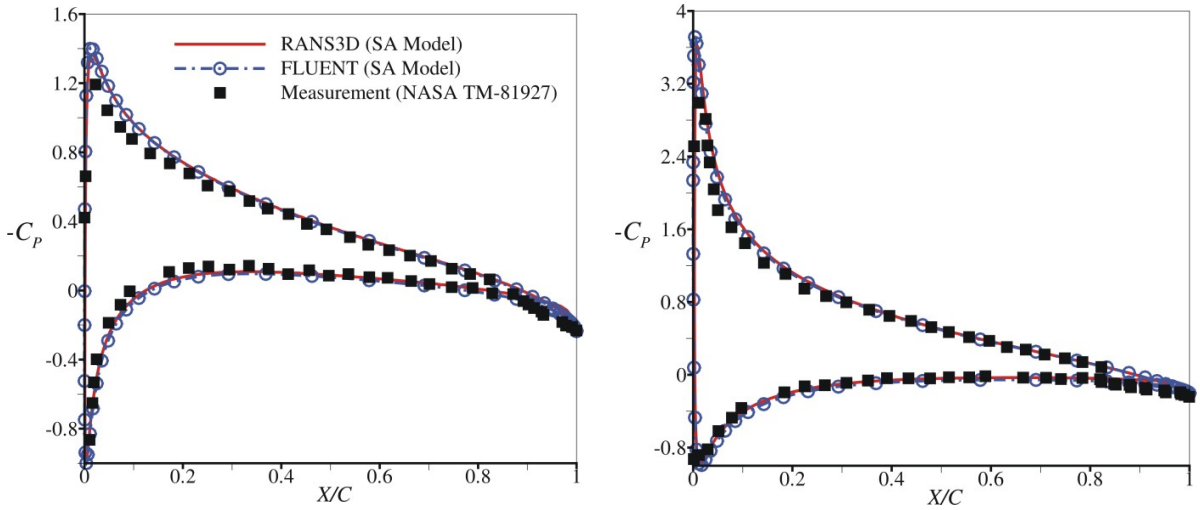

(a) α =4^0 (b) α =8^0

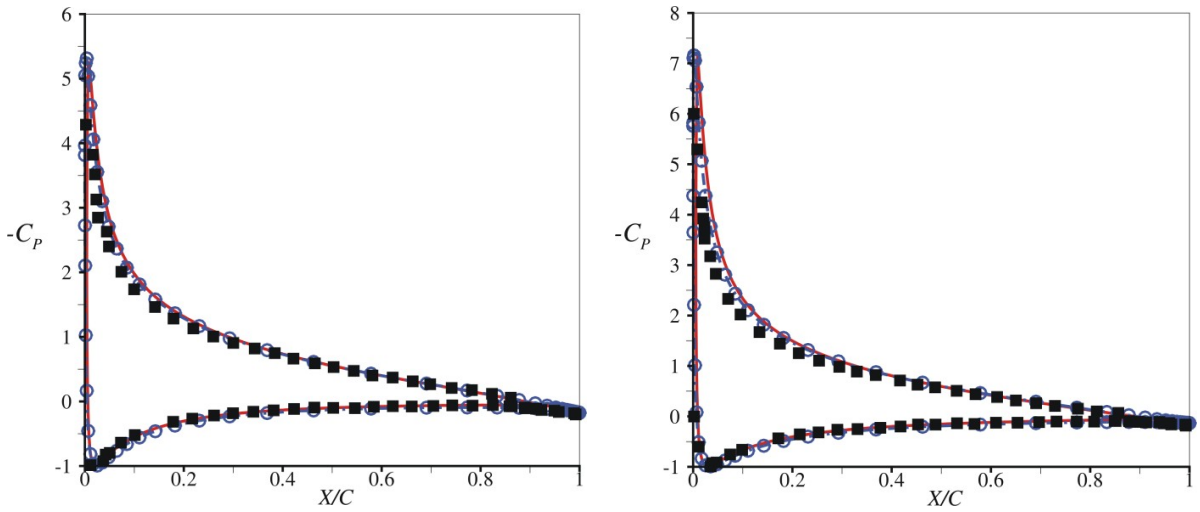

(c) α =10^0 (d) α =12^0

Figure 4.13: Variation of surface pressure coefficients for flow past NACA0012 Airfoil (Re=1.0x10^6, SA Turbulence Model)

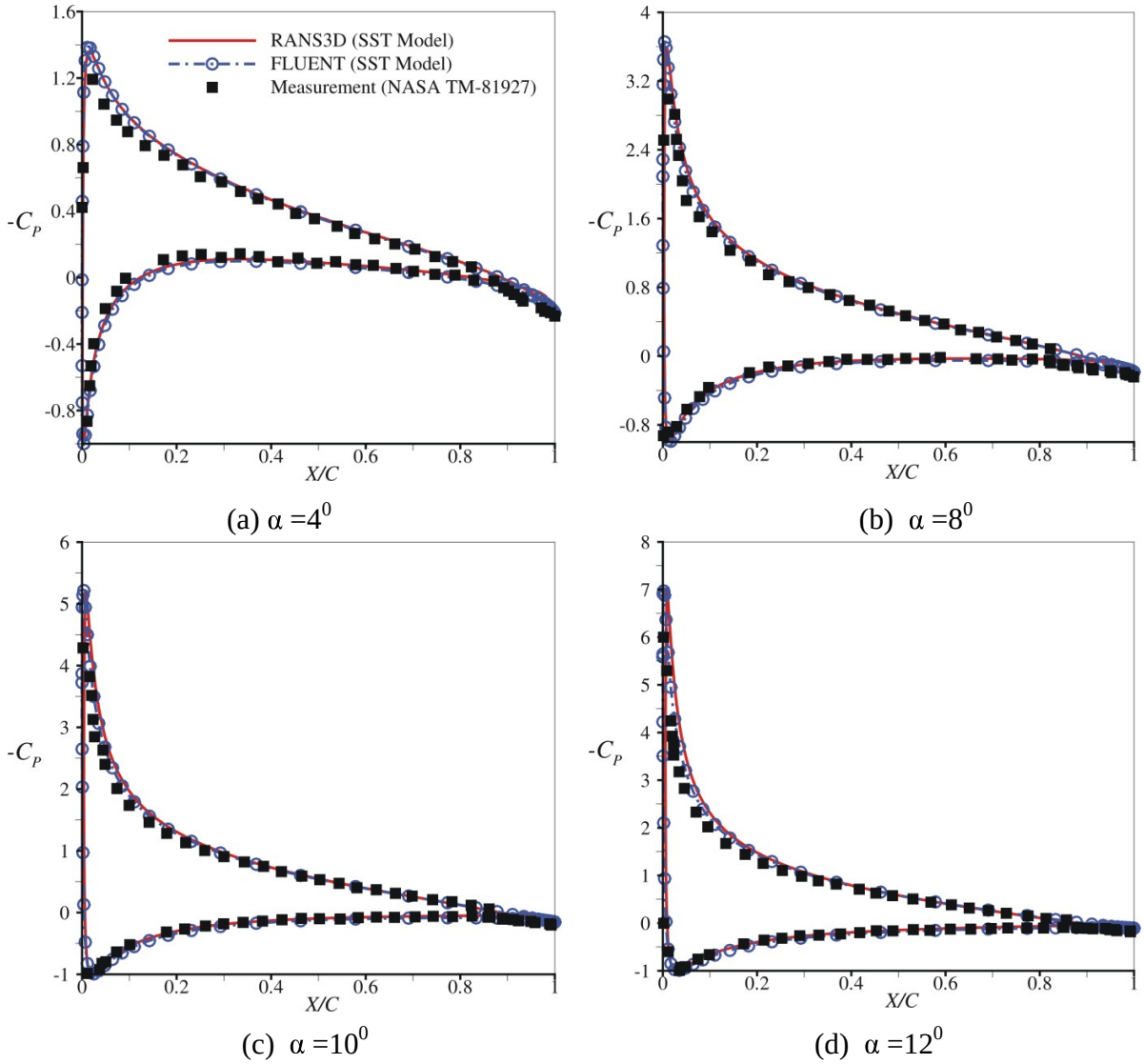

Figure 4.14: Variation of surface pressure coefficients for flow past NACA0012 Airfoil (Re=1.0x10^6 , SST Turbulence Model)

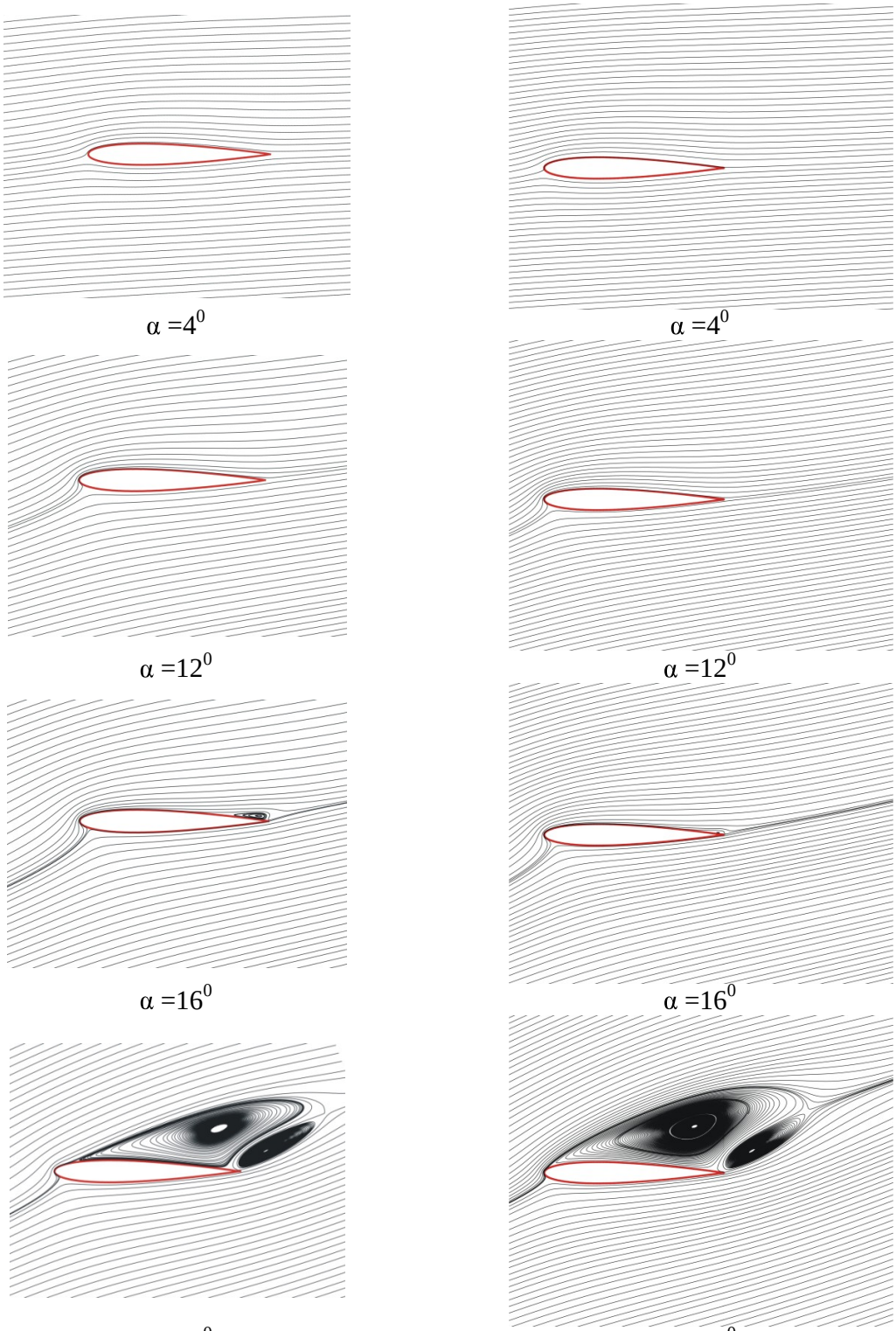

Figure 4.15: Computed streamlines for flow past NACA0012 Airfoil

(Re=1.0x10^{6,} SA Turbulence Model)

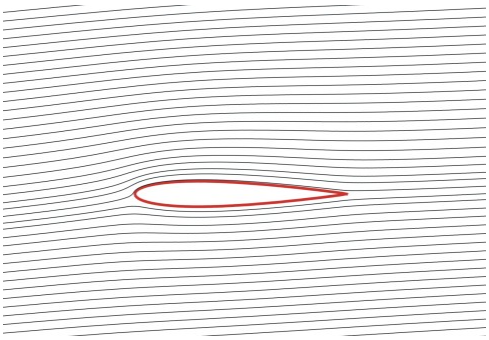

α =4^0

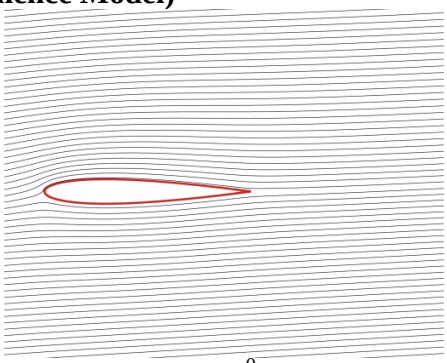

α =4^0

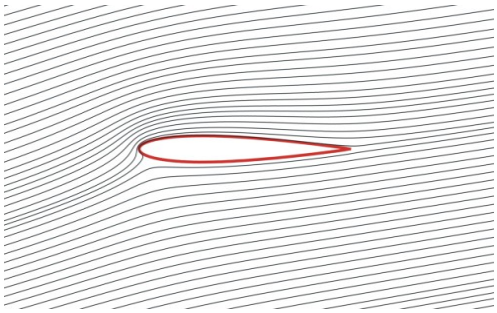

α =12^0

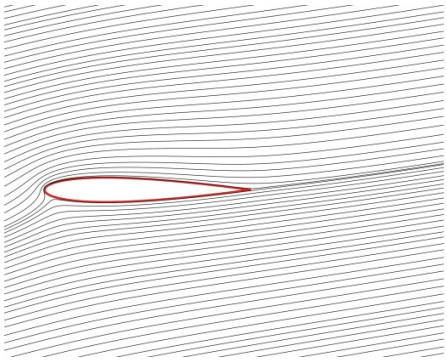

α =12^0

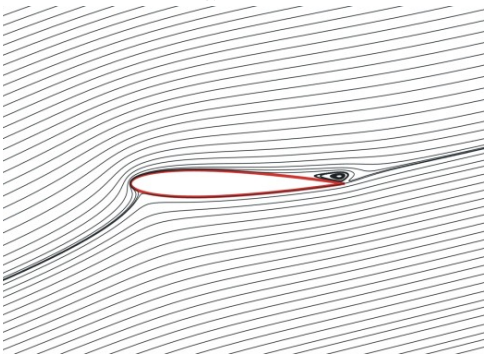

α =16^0

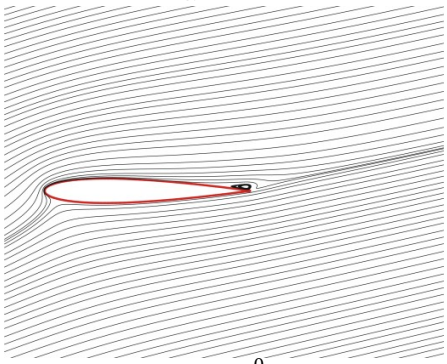

α =16^0

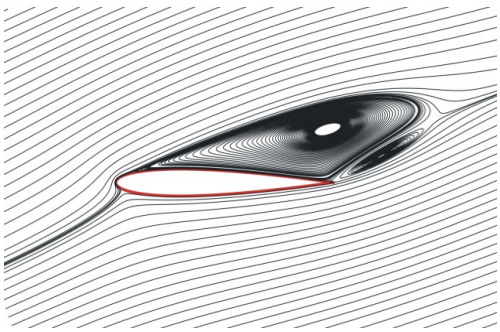

α =20^0
RANS3D

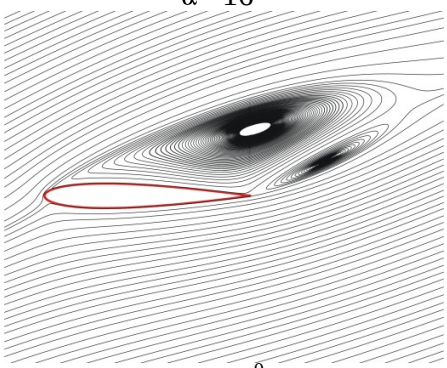

α =20^0
FLUENT

Figure 4.16: Computed streamlines for flow past NACA0012 Airfoil (Re=1.0x10^6, SST Turbulence Model)

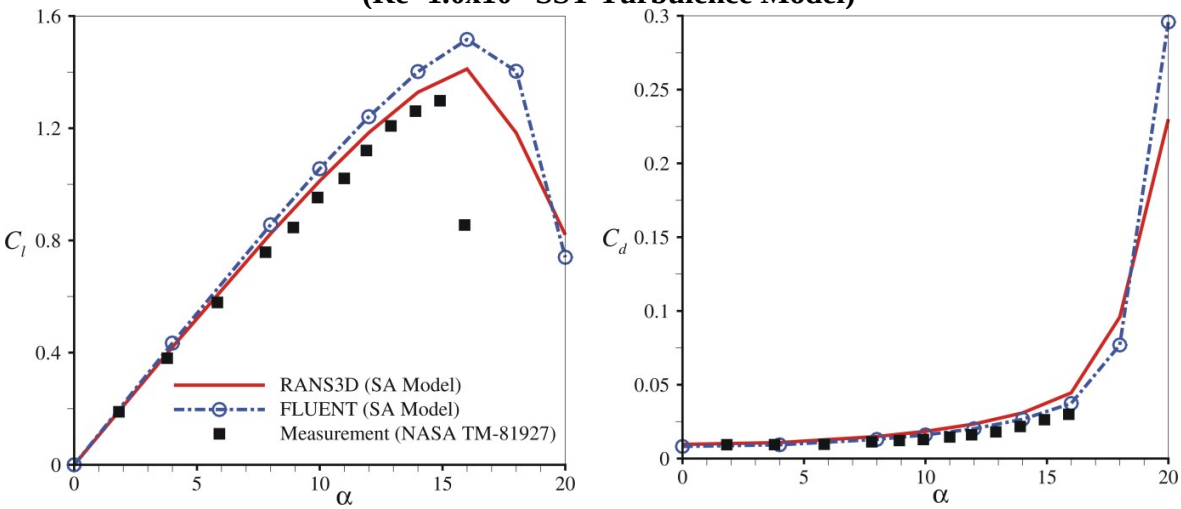

(a) Lift coefficient (b) Drag coefficient

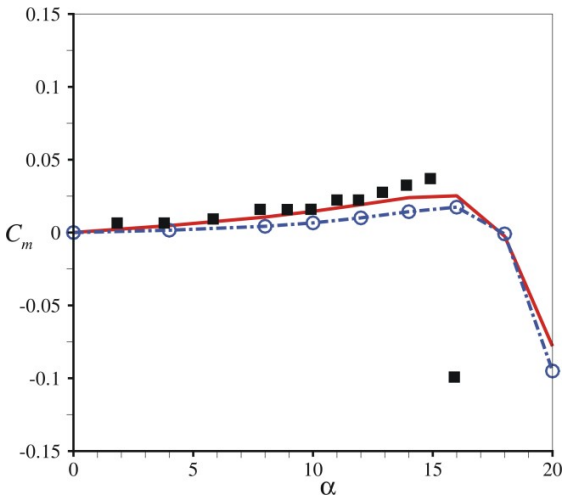

(c) Moment coefficient

Figure 4.17: Variation of Aerodynamic coefficients for flow past NACA0012 Airfoil (Re=1.0x10^6 , SA Turbulence Model)

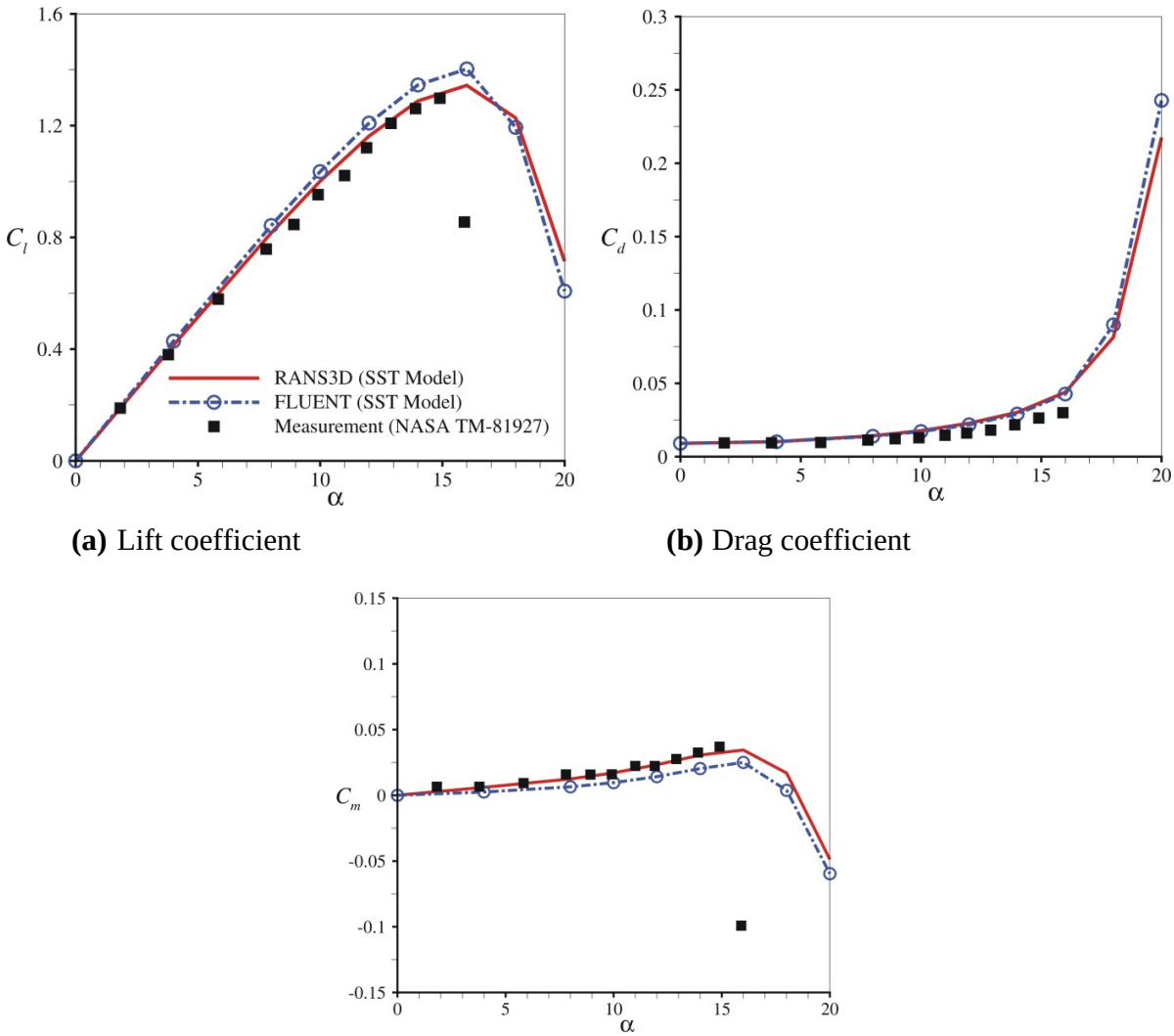

(a) Lift coefficient **(b)** Drag coefficient

(c) Moment coefficient

Figure 4.18: Variation of Aerodynamic coefficients for flow past NACA0012 Airfoil (Re=1.0x10^6 , SST Turbulence Model)

5. Conclusions

Performance of widely used CFD commercial code, namely FLUENT, and the in-house code RANS3D, is reported for a few simple benchmark flows. *viz.* laminar flow in a lid-driven square cavity, turbulent flow past a backward facing step and the turbulent flow past an aerofoil. The results obtained by both the codes for all the three different cases covering both laminar and turbulent flows are encouraging and shows a good agreement.

References

ANSYS Inc (2009), ANSYS FLUENT Solver Theory Guide

D.H.Charles, (1981), *Two-dimensional aerodynamic characteristics of the NACA0012 airfoil in the Langley 8-foot transonic pressure tunnel, NASA TM 81927*

Fathima, A., Baldawa, N.S., Pal, S., Majumdar, S., (1994), *Grid generation for arbitrary 2D configurations using a differential algebraic hybrid method,* NAL Project Document CF9416

Gianluca Iaccarino, (2000), *Prediction of the turbulent flow in a diffuser with commercial CFD codes,* Annual Research Brief, Center for Turbulence Research (CTR), Stanford University

Ghia, U., Ghia, K. N., Shin C.T., (1982), High-*Re solutions for incompressible flows using the Navier-Stokes equations and a multigrid method,* Journal of Computational Physics, 48, 387-411

Jovic., Driver., (1994), *Backwards-Facing Step Measurements at Low Reynolds Number, Reh=5000,* NASA TM 108807

Majumdar, S., (1988), *Role of under relaxation in momentum interpolation for calculation of flow with non-staggered grids,* Numerical Heat Transfer, vol. 13, pp. 125-132

Majumdar, S., Rajani, B. N., Kulkarni, D. S., Subrahmanya, M. B., (2010), *Numerical Simulation of Incompressible Turbulent Flow using Linear Eddy Viscosity-based Turbulence Models,* Defence Science Journal, vol. 60, n. 6, pp. 614-627

Menter, F. R., (1994), *Two-equation eddy-viscosity turbulence models for engineering application,* AIAA Journal, vol. 32, pp. 269-289

Patankar, S.V., Spalding, D.B., (1972), *A calculation procedure for heat, mass and momentum transfer in three-dimensional parabolic flows,* International Journal of Heat and Mass Transfer, vol. 15, pp. 1787-1806

Spalart, P. R., Allamaras, S. R., (1992), *A one-equation turbulence model for aerodynamic flow,* AIAA paper, vol. 92, no. 0439

Stone, H.L., (1968), *Iterative solution of implicit approximations of multidimensional partial differential equations,* SIAM Journal of Numerical Analysis, vol. 5, pp. 530-538

CFD SIMULATION USING FLUENT AND RANS3D

- A VALIDATION EXERCISE

Venkatesh Talupur Pradeep Shetty D.S.Kulkarni B.N.Rajani

NAL PDCF 1203

Computational and Theoretical Fluid Dynamics Division

National Aerospace Laboratories, Bangalore 560 017

May 2012

NATIONAL AEROSPACE LABORATORIES	DOCUMENTATION SHEET Class : Unrestricted No. of copies : 5

Title : CFD simulation using FLUENT and RANS3D – A validation exercise	
Author(s) : Venkatesh Talupur, Pradeep Shetty, D. S. Kulkarni, B. N. Rajani	
Division : CTFD	NAL Project No. : C-1-168
Document No. : PD CF 1203	Date of issue : May 2012
Contents : 18 Pages 18 Figures 1 Tables 12 References	
External Participation : Nil	
Sponsor : NPMICAV- ADE (DRDO), Bangalore	
Approval : Head, CTFD Division	
Remarks : Nil	
Keywords : RANS3D computation, FLUENT computation, Lid-driven cavity, Backward facing step, NACA0012 aerofoil	

Abstract :

The present work involves two-dimensional numerical simulation of three benchmark problems like (i) Laminar flow in a lid driven cavity (ii) Turbulent flow past a backward facing step and (iii) turbulent flow past NACA0012 aerofoil, using in-house flow solution code RANS3D and the commercially available FLUENT code. The results obtained using these codes are compared with the available measurement data and/or other computations.